# Demagnetization of a Complete Superconducting Radiofrequency Cryomodule: Theory and Practice

Saravan K. Chandrasekaran*, Anthony C. Crawford*

*Fermilab, Batavia, IL 60510, USA

**A significant advance in magnetic field management in a fully assembled superconducting radiofrequency (SRF) cryomodule has been achieved and is reported here. Demagnetization of the entire cryomodule after assembly is a crucial step toward the goal of average magnetic flux density less than 0.5 μT at the location of the superconducting radio frequency cavities. An explanation of the physics of demagnetization and experimental results are presented.**

***Index Terms*— SRF, cryomodule, demagnetization**

## I. Introduction

The recent advent of extremely low surface resistance, nitrogen-doped niobium superconducting radio frequency (SRF) cavities [1] has led to a redoubling of the effort to prevent magnetic flux from being trapped in the niobium during transition from the normal to the superconducting state at the critical temperature ($T_c$) for niobium of 9.25 K. Trapped magnetic flux in the thin layer that supports SRF current results in increased Ohmic losses that are the largest single contribution to residual resistance [2] for cavities prepared with state of the art techniques. For continuous wave (CW) operation the added resistance causes a significant increase in thermal power that must be removed, at high cost, by a liquid helium refrigerator, typically operating at 2 K. It is therefore possible for an accelerator project to realize considerable savings in equipment and operating funds by minimizing trapped magnetic flux.

Residual resistance due to trapped magnetic flux is larger for nitrogen-doped SRF cavities than for pure niobium cavities [3], thereby increasing the importance of careful magnetic management. Flux trapping in niobium is a complex phenomenon and a function of many variables. The most prominent sources for trapped flux and their appropriate means of mitigation are diagrammed in Fig. 1. Background information is available for the sources: ambient field [4], magnetization [5], and Seebeck voltage driven thermocurrent [6], as well as for flux expulsion [7], [8].

Elliptical multicell cavities, when installed within their helium vessels, tend to take the form of an electrical coaxial transmission line [6]. The cavity and the helium vessel are welded together in a bi-metallic junction at both ends of the cavity. The cavity and the helium vessel are typically made from different materials: niobium for the cavity and titanium for the helium vessel. The temperature dependent Seebeck coefficients for niobium and titanium differ significantly. This means that the cavity-helium vessel system behaves like a pair of thermocouple junctions. If there is a temperature difference between the two ends of the cavity, there will be an electromotive force that drives a continuous current along the cavity and that returns in the helium vessel. If the temperature and current distributions are not axially symmetric, there will be a resulting magnetic flux density at the cavity RF surface that can be "frozen in" during $T_c$ transition. For the case of horizontal orientation, the bottom of the cavity typically transitions through $T_c$ first, breaking the axial symmetry. One way to prevent thermocurrent flux is to cool the cavity through $T_c$ with no temperature gradient in the axial direction, thus preventing any thermocurrent. However, developing a unidirectional axial thermal gradient ($dT/dx$) greater than 20 K/m at $T_c$ is the most effective means of expelling flux [8].

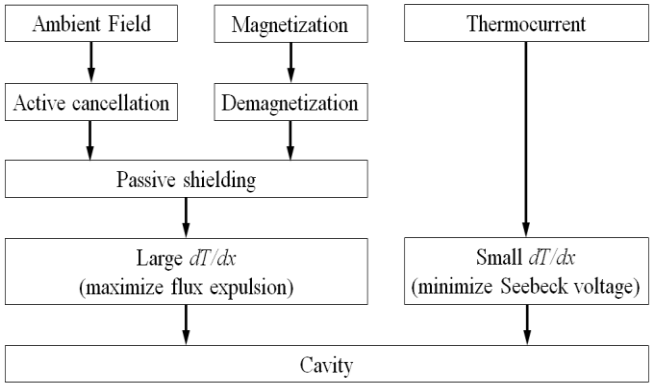


Fig. 1. Sources of trapped magnetic flux and their means of mitigation. Sources are in the top row and mitigation is placed between the source and the cavity.

Optimal arrangements for flux expulsion and thermocurrent management are being actively studied at the present time. If the thermocurrent electrical circuit can be broken by a ceramic insulator, or equivalent means, then the problem of frozen flux from thermocurrent sources can be eliminated, allowing for more liberal experimentation with the thermal spatial gradient required for efficient flux expulsion. Not all sheet niobium used for SRF cavities expels flux efficiently. Furnace annealing at temperatures exceeding 900 C is required in some cases [9]. Until the time arrives when the flux expulsion technique is mature, and is proved reliable when applied to cavities with

Fermilab is operated by Fermi Research Alliance, LLC under Contract No. De-AC02-07CH11359 with the United States Department of Energy.

their axis in the horizontal orientation, the lowest probability for increased surface resistance due to flux trapping is to be realized by minimizing the magnetic flux density from ambient sources and magnetized components. Effective means of treating ambient sources are developed in Ref. [4]. The remainder of this report concentrates on the subject of demagnetization.

## II. Demagnetization

In SI units, the relationship between applied magnetic field (**H**), magnetic flux density (**B**), and magnetic moment per unit volume (**M**) is:

$$\mathbf{B} = \mu_0(\mathbf{H} + \mathbf{M}) \quad (1)$$

This allows for clarification of the term "demagnetization." A material in a demagnetized state should have **B**=0 when **H**=0. According to (1), this means that **M**=0 when **H**=0 for a demagnetized material. In order for total magnetization to be zero, the vector sum of all individual magnetization vectors from each magnetic domain in the material sample must be zero. While achievable under certain conditions, it will be shown that this state is not optimal for the purpose of magnetic shielding, including magnetic shielding for SRF cryomodules. In this report, an object that is demagnetized according to the definition presented above, and that has zero remanence **M**=0 when **H**=0, will be referred to as "demagnetized." An object that has undergone a demagnetization procedure, but that has remanent magnetization **M**≠0 when **H**=0, will be referred to with the use of Italicized letters: "*demagnetized*."

One way of *demagnetizing* is to slowly diminish the magnitude of the AC current in the circuit shown in Fig. 2. The object being *demagnetized* is a cylinder inside a solenoidal coil. For our case of special interest, the object would be a complete SRF cryomodule, approximately 11.4 m in length and 1 m in diameter. The geometry of our SRF cryomodule is that of thin walled cylinders placed inside thin walled cylinders, all with their axes pointing in the same direction. So, the basic problem is that of a thin walled cylinder immersed in an axial magnetic field.

In practice, when we *demagnetize* a cryomodule, it is immersed in a steady state ambient field due to the local Earth magnetic field, with its associated perturbations and irregularities. Thus the total applied field $\mathbf{H}_{total}$ has a decreasing AC component from a power source and a constant DC component from the environment, $\mathbf{H}_{DC}$. The effective applied field looks like Fig. 3. If $\mathbf{H}_{DC}$=0, then the cryomodule would, in principle, be truly demagnetized according to the definition presented previously.

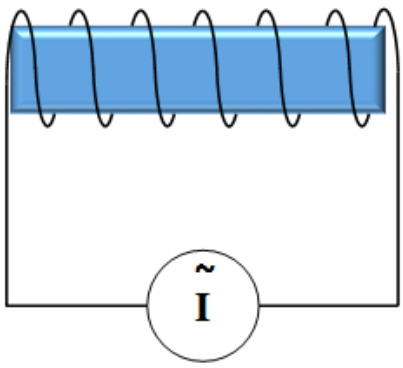


Fig. 2. The concept for *demagnetization*.

Another way of *demagnetizing* is to heat the material to a state above the Curie temperature. This, in addition to grain growth, is one of the goals of magnetic annealing performed by magnetic shield vendors. If $\mathbf{H}_{DC}$=0 during the cool down of the material, it will be demagnetized when it reaches room temperature. If $\mathbf{H}_{DC} \neq 0$ then the material will acquire overall magnetization as it cools, provided that the cooling is not faster than the time required for magnetic domain formation and ordering. The reason that magnetization happens is that a partial ordering of magnetization vectors with the applied field minimizes the free energy of the magneto-thermodynamic system. It is likely that commercially available, heat treated Cryoperm and Permalloy80 both have some amount of remanent magnetization following furnace treatment. We will see that induced remanence due to $\mathbf{H}_{DC}$ has a significant effect on apparent magnetic shielding efficiency.

## III. Modeling Aftereffects of *Demagnetization*

What is the arrangement of magnetic flux lines in the vicinity of a thin walled, open ended cylinder following *demagnetization*? A working model for *demagnetization* should include both ambient environmental magnetic field and remanent magnetization within the shield material. A means of including remanence has been missing from previous cryomodule studies, and will be developed here.

The approximate geometry for an International Linear Collider (ILC) cryogenic magnetic shield, without end caps, is used for the purpose of illustrating an example of a thin walled cylinder. Applied field will be in the axial direction of the cylinder, as this is the most critical case for attenuation of magnetic flux for SRF cavities. The results will be applicable to the general case of thin walled cylinders, with appropriate modification of geometry and material parameters.

We assume that the magnitude of $\mu_0\mathbf{H}_{DC}$ in Fig. 3 is 50 μT (500 mG), a value that is approximately the largest expected for a horizontal component of the Earth field. The field is uniform

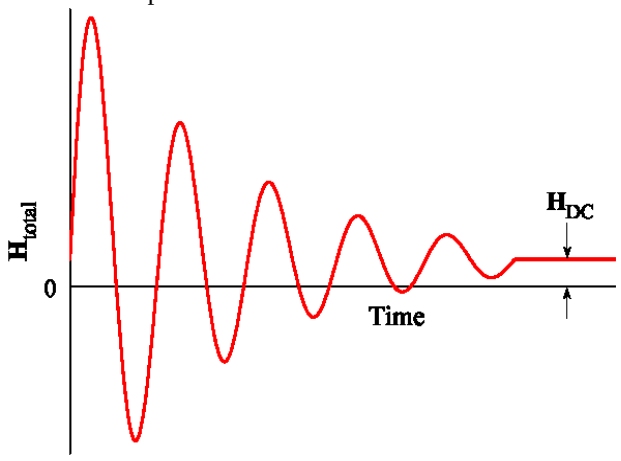


Fig. 3. *Demagnetization* in an ambient field.

when the magnetic material is not present. Prior to the *demagnetization* procedure, there is no remanent magnetization in the magnetic material. What is the magnetic flux line distribution near the ferromagnetic material when it is immersed in the previously uniform field? Results are shown in Fig. 4 for the following values: cylinder inner radius=127 mm, wall thickness=1 mm, relative permeability=$\mu_r$=100,000. The assumed value for $\mu_r$ is not unreasonably high for an undamaged cylinder made from annealed Cryoperm or Permalloy80. There is symmetry under the operation of rotation about the Z axis in Fig. 4. For this simple model, the material permeability is assumed to be constant. The results are qualitatively similar to the case of the steel vacuum vessel of the cryomodule, which also has a thin walled cylindrical geometry, albeit on a larger scale. The relative permeability of the steel pipe would be in the range 300 to 500.

What is the flux distribution within the walls of the cylinder? The Z component of the magnetic flux density is plotted from cylinder point **A** to point **B** as the red curve in Fig. 5. The radial coordinate for the plot in Fig. 5 is 127.5 mm, the midpoint of the cylinder walls.

After *demagnetization*, the cylinder will be left with a remanent magnetization that is similar to, but of smaller magnitude than, the magnetization due to $\mathbf{H}_{DC}$. The flux density in the cylinder wall under the applied field is small and does not approach the saturated limit for Cryoperm of approximately 0.7 T, but there will be remanence, nonetheless. During experiments at Fermilab, changes in magnetic flux density of 0.5 μT (5 mG) have been observed along the axis of Cryoperm

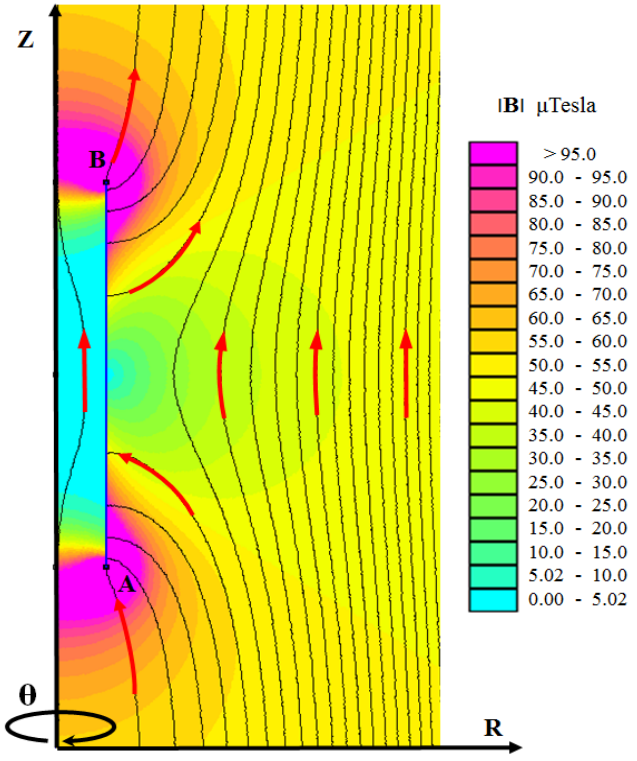


Fig. 4. A high permeability cylinder immersed in a uniform magnetic field of magnitude $\mu_0|\mathbf{H}|$=50 μT (500 mG). Arrows indicate the direction of the flux lines.

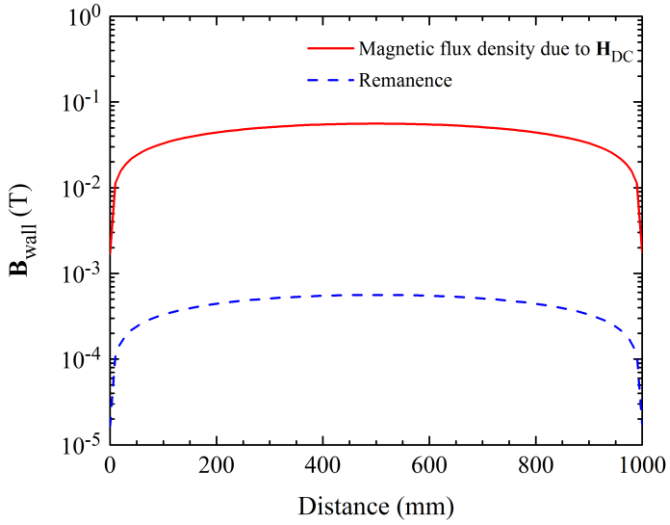


Fig. 5. Magnetic flux density distribution in the cylinder wall due to an ambient field of $\mu_0|\mathbf{H}|$=50 μT, along with the modeled remanence. Only the Z component of the field is plotted in each case.

cylindrical shields installed in a steel cryomodule vacuum vessel following *demagnetization* procedures. This subject is further discussed in Ref. [5]. Flux density changes of this type are due to remanence and occur if the AC *demagnetization* cycle of Fig. 3 is terminated at too large a field value, for example, above 2 A-turns/m peak value for the concluding AC cycle. In order to further understand this observed effect, we proceed to develop a model of remanence in the cylinder wall that produces axial magnetic flux density changes of 0.5 μT. We will then investigate the implications of remanence magnetization for magnetic shielding efficiency.

With proper choice of current density, a remanence model based on thin current sheets of equal magnitude, but opposite polarity, located on the inner and outer radii of the cylinder duplicates the magnetic flux density distribution due to $\mathbf{H}_{DC}$ of Fig. 4. The current in the sheets is then reduced until stray flux density from the cylinder measured along the axis is 0.5 μT (5 mG). This forms the basis for a model for remanence in the magnetic shield. The remanence in the cylinder wall that produces a 0.5 μT (5 mG) central flux density is shown as a blue colored dashed curve in Fig. 5.

The axial flux density for this model is plotted in Fig. 6. The associated flux density map is shown in Fig. 7. The reader should pay special attention to the flux lines that return to the opposite pole within the interior of the cylinder in Fig. 7. These will play an important role in the ability of the shield to attenuate ambient field.

The model for internal magnetization after *demagnetization* now allows for investigation of the shielding efficiency of the cylinder. The following cases are considered:

1. Remanence Aligned: The cylinder is immersed in the 50 μT ambient magnetic flux density in which it was *demagnetized*.
2. No Remanence: A truly demagnetized cylinder, with zero remanence, placed in a 50 μT ambient magnetic flux density.

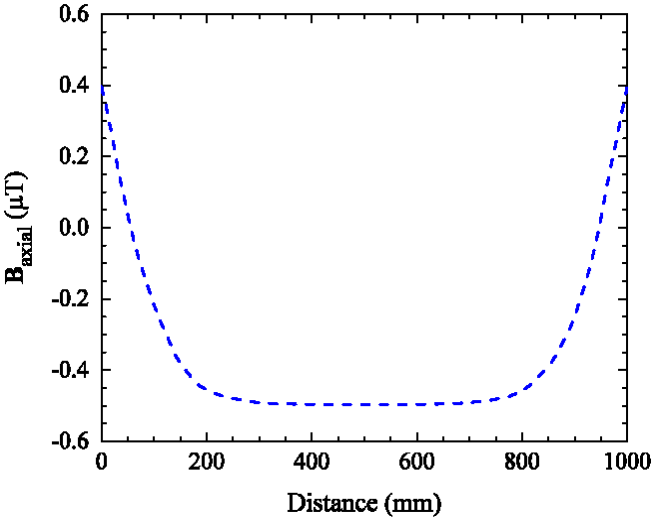


Fig. 6. Magnetic flux density along the axis of the magnetized cylinder due to remanence.

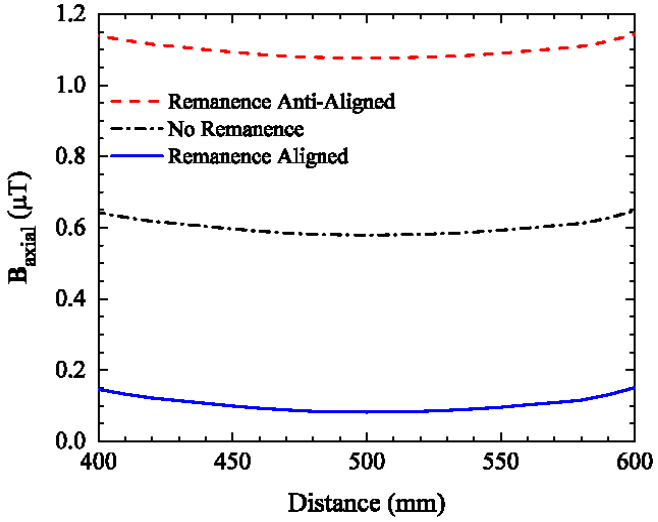


Fig. 8. Attenuated magnetic flux density for different orientations of remanence.

3. Remanence Anti-Aligned: The cylinder is immersed in a 50 μT ambient magnetic flux density of equal magnitude, but opposite direction, from that in which the cylinder was *demagnetized*.

The magnetic flux density along the cylinder axis is shown in Fig. 8 for each of the three cases. Distance is measured from the end of the open cylinder. The reader should note that there are large values of flux density near the ends of the open cylinder. These values diminish exponentially with distance along the cylinder axis toward the midpoint. It is the central portion of the length of the cylinder that is important to us here and that is indicative of the shielding efficiency of the material. A view of only the central portion of the cylinder is shown in the figure. In a real cryomodule, end effects would be mitigated by the use of end caps on the cylinder, i.e., a local reduction in radius.

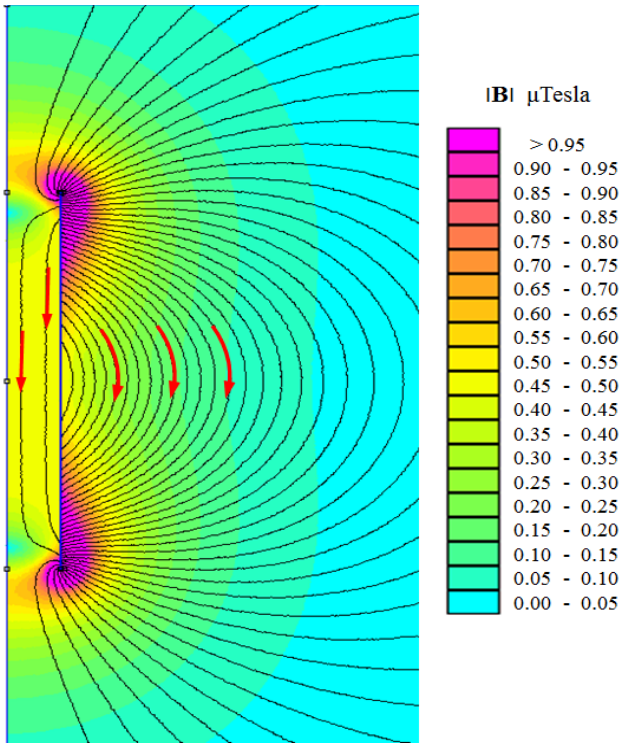


Fig. 7. Magnetic flux density originating from the magnetized cylinder. Arrows indicate the direction of the flux lines.

## IV. Practical Implications of the Model

The best result for flux reduction at the SRF cavities is obtained by optimizing remanence and not from true demagnetizing. This is due to the remanence induced stray flux lines that return through the interior volume of the hollow cylinder. The flux return pattern within the interior volume of the hollow cylinder matters a great deal for shielding applications. The principle of linear superposition for magnetic field allows the following argument: When flux lines due to remanence within the cylinder wall are in the same direction (aligned) as those from the applied external field, the flux lines due to remanence that return through the hollow interior are in the opposite direction from the lines in the interior due to the applied field, resulting in smaller total flux magnitude. In the opposite case (anti-aligned), the returning flux lines from the remanence will add to those from the applied field.

An initial *demagnetization* of the low carbon steel vacuum vessel is desirable. The reason is to eliminate localized areas of large remanent flux density (values as high as 1 mT) that are present after fabrication operations of welding, bending, and handling of parts with electromagnets. High applied field (650 A-turns/m) is essential to *demagnetize* these areas. However, the optimization of remanence with respect to the local ambient environment may be achieved with applied field lower than this value and can be done after the cryomodule is fully assembled.

## V. Experimental Demagnetization of a Cryomodule

The cryomodule shown in Fig. 9 was instrumented with an array of thirteen internal magnetometers. Unacceptably large changes in flux density, measured by these instruments, appeared after a welding operation to cryogenic fluid handling components. This welding operation was one of the final steps before completion of the cryomodule. It was decided to perform *demagnetization* before proceeding with the cryomodule.

Table 1 lists the readings of the magnetometers before and after two different 350 A-turns/m remedial *demagnetization* procedures. The first *demagnetization* of the complete cryomodule was performed at Work Station 5 (WS5) in the Industrial Center Building at Fermilab. Work Station 5 is the final assembly point for the cryomodule. The orientation of the cryomodule for *demagnetization* and measurement was east-to-west at WS5. The second complete cryomodule *demagnetization* was performed after the cryomodule had been transported a distance of approximately 2 kilometers and installed within a radiation shielding cave at Cryomodule Test Stand 1 (CMTS1) at Fermilab. There, the orientation was north-to-south, with ambient magnetic environment significantly different from WS5.

Magnetometers numbered 1 through 8 represent a mixed sampling of transverse and axial flux density components and were located in the space between the outer cavity wall and the inner wall of the helium vessel for four of the eight cavities in the cryomodule. Magnetometers 9 through 13 measure flux density in the axial direction and were located in the space between two layers of passive shielding around the outside of the helium vessel for five of the cavities. The magnetometers used were Bartington single axis fluxgates, model MAG-F, packaged for cryogenic applications. Their uncertainty is less than ± 0.01 μT. All readings were taken at room temperature (approximately 293 K).

From Table 1 we see that flux density with magnitude as high as 4.1 μT (41 mG) is reduced to the level of 0.1 μT (1 mG) by the *demagnetization* procedure at WS5. Indeed, there are no readings greater than 0.23 μT (2.3 mG) following *demagnetization*. It should be re-emphasized that the improvement is due to two different phenomena that proceed simultaneously during cryomodule *demagnetization*: (1) the reduction of local areas of large magnitude remanence in the cryomodule, in this case, from a welding operation, and (2) the adjustment of the cryomodule remanence to the local ambient environmental field. For the *demagnetization* example presented in this report, it is estimated that effect (1) was responsible for reducing magnetic flux density readings to the level of 0.5 μT (5 mG) and (2) was responsible for further reduction to the level of 0.2 μT (2 mG). Evidence for this claim is to be found in the magnetometer readings at CMTS1 in Table 1. The largest difference in the magnetometer readings before and after the move from WS5 to CMTS1 appears on magnetometer number 8, a change of +0.42 μT (4.2 mG), resulting in a reading of +0.350 μT (3.5 mG). The change can be due to the different magnetic environment at CMTS1, from mechanical shock during transportation, or a combination of both. If an easily magnetized ferromagnetic object, in this case, the steel vacuum pipe, receives a sufficiently large mechanical shock, some of the magnetic domains will align themselves with the local ambient magnetic field. This reaction to mechanical stimulation is similar to realignment due to the magnetic stimulation of a *demagnetization* procedure. The domain arrangement of the ferromagnetic object under shock adjusts itself to the lowest achievable free energy state for its ambient magnetic environment at the time of the shock. *Demagnetization* 2 at CMTS1 then re-adjusts the domains to the environment at CMTS1. The final reading on magnetometer number 8 is -0.015 μT (0.15 mG). The largest measured magnitude of flux density in the cryomodule after *demagnetization* 2 is 0.143 μT (1.4 mG).

TABLE 1
Magnetic Flux Density Measurements (in Units of μT)

| Magnetometer Number | **B** before *Demag.*1 at WS5 | **B** after *Demag.*1 at WS5 | **B** before *Demag.*2 at CMTS1 | **B** after *Demag.*2 at CMTS1 |
|---|---|---|---|---|
| 1 | -0.036 | -0.043 | -0.219 | -0.125 |
| 2 | -0.218 | +0.039 | +0.260 | -0.143 |
| 3 | -0.089 | -0.098 | +0.162 | -0.066 |
| 4 | -4.109 | -0.039 | +0.222 | -0.029 |
| 5 | -0.110 | +0.011 | -0.033 | -0.005 |
| 6 | +2.644 | +0.032 | -0.228 | +0.014 |
| 7 | +0.195 | -0.035 | +0.057 | -0.023 |
| 8 | -4.014 | -0.070 | +0.350 | -0.015 |
| 9 | -0.133 | +0.227 | -0.049 | +0.122 |
| 10 | -0.013 | +0.071 | -0.072 | +0.067 |
| 11 | +0.254 | +0.051 | +0.018 | +0.096 |
| 12 | +0.117 | +0.060 | +0.087 | +0.060 |
| 13 | -0.358 | +0.099 | +0.070 | +0.024 |

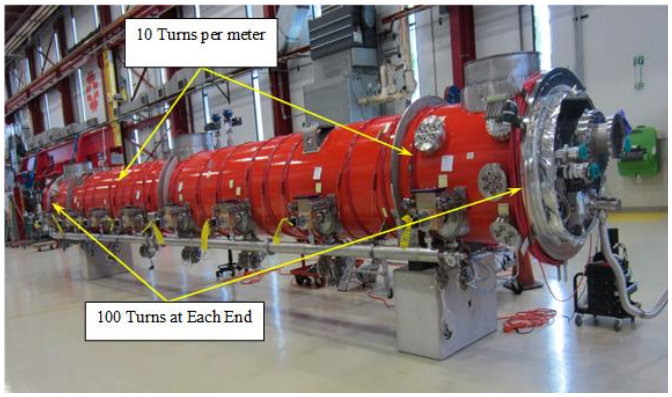


Fig. 9. The cryomodule with *demagnetization* coils in place at WS5.

## VI. Active Cancellation

It should be noted that the ambient axial magnetic flux densities at both WS5 and CMTS1 are favorable for achieving low readings on axial magnetometers 9 through 13. The axial flux density at WS5 was low, less than 10 μT (100 mG). The axial magnetic flux density at CMTS1 reverses direction within the space occupied by the cryomodule, thus preventing flux concentration in the walls of the cylindrical shields near the midpoint of the cryomodule, as described in Ref. [4]. The

readings for axial flux density in Section V are therefore likely to be lower than can be expected as an average for cryomodules in other locations. As a result, it is not possible to state that active cancellation will be unnecessary for cryomodules in their final location in a linac. A *demagnetized* cryomodule subjected to a uniform 20 μT (200 mG) axial field will benefit significantly from active axial cancellation.

Could the benefit of active cancellation be realized by intentionally magnetizing the cryomodule in the favorable axial direction? The answer is, yes, and this has been done experimentally at Fermilab with small sample cylinders as well as with a partially assembled full scale cryomodule that consisted of a 12 m long steel vacuum pipe equipped with eight single layer Cryoperm cavity shields [10]. This technique allows extremely low axial flux density with the active cancellation coils de-energized. However, the same measurements, instrumentation, coils, and power supplies are required for either case, so the choice of which technique to use is a matter of preference whether to rely on field from an electric current source or from remanence created by a deliberate and careful arrangement of magnetic domains.

## VII. Conclusion

Stray flux lines from remanent magnetization in a thin walled ferromagnetic cylindrical shield adds vectorially to the attenuated ambient flux at the location of the object that is to be shielded. In situ *demagnetization* optimizes the remanent field in the cylinder wall for shielding purposes. If the magnetic environment of a cryomodule is changed, it will be beneficial to repeat the demagnetization procedure for the new environment. These effects have now been successfully demonstrated in a fully assembled 11.4 m cryomodule and *demagnetization* is seen to be an essential step in achieving satisfactorily low flux density for nitrogen-doped cavities until the time arrives when flux expulsion technology has been perfected for SRF cryomodules.

## Acknowledgment

An effective and affordable polarity reversing power supply was created to match the requirements of this project by M. Matulik and M. Cherry of the Fermilab Particle Physics Division. A description of this device will appear in a future publication. A fully detailed description of the specific techniques involved in *demagnetization* of the cryomodule shown in Fig. 9 is forthcoming.

## References

[1] A. Grassellino, A. Romanenko, O. Melnychuk, Y. Trenikhina, A. Crawford, A. Rowe, M. Wong, D. Sergatskov, T. Khabiboulline, and F. Barkov, "Nitrogen and Argon Doping of Niobium for Superconducting Radio Frequency Cavities: A Pathway to Highly Efficient Accelerating Structures," Supercond. Sci. Technol. 26, 102001 (2013). http://dx.doi.org/10.1088/0953-2048/26/10/102001

[2] H. Padamsee, J. Knobloch, and T. Hays, *RF Superconductivity for Accelerators*, (Wiley, New York, 1998) p. 173.

[3] D. Gonnella, *The Fundamental Science of Nitrogen-Doping of Niobium Superconducting Cavities*, Ph.D. dissertation, Cornell Univ., Ithaca, NY, 2016, p.140. http://www.classe.cornell.edu/rsrc/Home/Research/SRF/SrfDissertations/DanielGonnellaThesis_final.pdf

[4] "The Conceptual Design Report for the TeSLA Test Facility Linac: Version 1.0", 1995, p.160. http://tesla.desy.de/TTFReport/CDR/pdf/cdrchap4.pdf.

[5] A. Crawford, "In Situ Cryomodule Demagnetization", arXiv:1507.0658

[6] A. Crawford, "A Study of Thermocurrent Induced Magnetic Field in ILC Cavities", arXiv:1403.7996

[7] M. Martinello, M. Cecchin, A. Grassellino, A. Crawford, O. Melnychuk, A. Romanenko, D. Sergatskov, ``Magnetic Flux Studies in Horizontally Cooled Elliptical Superconducting Cavities", J. Appl. Phys. 118, 044505 (2015); http://dx.doi.org/10.1063/1.4927519

[8] A. Romanenko, A. Grassellino, A. C. Crawford, D. A. Sergatskov, and O. Melnychuk, "Ultra-high Quality Factors in Superconducting Niobium Cavities in Ambient Magnetic Fields up to 190 mG" Appl. Phys. Lett. 105, 234103 (2014). http://dx.doi.org/10.1063/1.4903808

[9] S. Posen, M. Cecchin, A. Crawford, A. Grassellino, M. Martinello, O. Melnychuk, A. Romanenko, D. Sergatskov, Y. Trenikhina, "Efficient Expulsion of Magnetic Flux in Superconducting Radiofrequency Cavities for High $Q_0$ Applications", J. Appl. Phys. 119, 213903 (2016); http://dx.doi.org/10.1063/1.4953087

[10] A. Crawford, Fermilab, unpublished.